



## Sucrose solutions alter the electric capacitance and dielectric permittivity of lipid bilayers

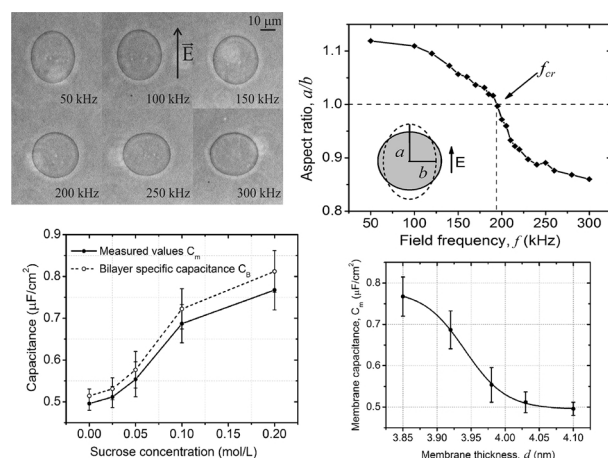
Victoria Vitkova<sup>a,\*</sup>, Denitsa Mitkova<sup>a,c</sup>, Krassimira Antonova<sup>a</sup>, George Popkirov<sup>b</sup>,  
Rumiana Dimova<sup>c,\*</sup>

<sup>a</sup> Institute of Solid State Physics, Bulgarian Academy of Sciences, 72 Tzarigradsko Chaussee Blvd., 1784 Sofia, Bulgaria

<sup>b</sup> Central Laboratory of Solar Energy and New Energy Sources, Bulgarian Academy of Sciences, 72 Tzarigradsko Chaussee Blvd., 1784, Sofia, Bulgaria

<sup>c</sup> Max Planck Institute of Colloids and Interfaces, Science Park Golm, 14424, Potsdam, Germany

### GRAPHICAL ABSTRACT



### ARTICLE INFO

#### Keywords:

Capacitance  
Dielectric permittivity  
Lipid bilayers  
Giant vesicles  
Electrodeformation  
Sucrose

### ABSTRACT

Understanding sugar-membrane interactions is of fundamental and technological relevance considering the role of sugars in drought-protection mechanisms of plants as well as the cryo- and bio-preserving effect of carbohydrates in many industrial and medical applications. In this work, we investigated the effect of sucrose on the electrical properties of membranes. In particular, we measured the specific capacitance of palmitoyl-oleoyl phosphatidylcholine membranes in aqueous solutions of sodium chloride. Different concentrations of sucrose were examined. The capacitance was assessed from the frequency-dependent deformation of giant unilamellar lipid vesicles in alternating electric field. Our measurements on giant vesicles in sugar-free aqueous solutions yield lower specific capacitance compared to values obtained for suspended and supported bilayers. This might be a result of the higher membrane tension in the latter systems, which is coupled to smaller thickness of the bilayer. We also report an increase of the bilayer capacitance upon increasing the sugar content in water. This finding is consistent with the sugar-induced thinning of membranes reported in the literature. However, the thinning is not sufficient to explain the observed capacitance increase with rising sugar concentration. We interpret the trend as resulting from an increase in the membrane dielectric permittivity.

\* Corresponding authors.

E-mail addresses: [viktoria@issp.bas.bg](mailto:viktoria@issp.bas.bg) (V. Vitkova), [rumiana.dimova@mpiikg.mpg.de](mailto:rumiana.dimova@mpiikg.mpg.de) (R. Dimova).

<https://doi.org/10.1016/j.colsurfa.2018.05.011>

Received 19 March 2018; Received in revised form 4 May 2018; Accepted 4 May 2018  
0927-7757/ © 2018 Elsevier B.V. All rights reserved.

## 1. Introduction

Synaptic activity and transmission of electrical impulses strongly depend on and are defined by the electrical properties of biological membranes the detailed characterization of which underlies the understanding of the governing mechanisms involved in such cellular processes. Research in this direction is also necessitated by numerous biomedical applications based on electroporation of membranes such as in gene and drug delivery, cancer treatment (as in electrochemotherapy) and cell-cell hybridization [1]. The response of cells to electric fields is to a larger extent governed by the cell membrane which encloses the cell and isolates it from the outside. The lipid bilayer, which is the main structural entity of biomembranes, is impermeable to ions. Thus, it behaves as a capacitor that strongly influences the electric field distribution in the cell. The investigation of the lipid bilayer capacitance and its dependence on external factors is necessary for the evaluation of the charging time of membranes and the membrane-field interactions [2]. The charging time, on the other hand, defines the transmembrane potential built-up across the membrane as charges start accumulating on both sides of the bilayer [3]. The transmembrane potential difference effectively induces electrical tension which can lead to deformation and poration of the cell. Thus, understanding the overall response of cells and membranes requires knowledge of fundamental electrical properties such as the membrane capacitance.

Various methods have been established for the measurement of the membrane capacitance. These include dielectric spectroscopy, the patch-clamp technique, as well as electromechanical methods exploiting single cell electrophoresis and electroporation, see e.g. [4]. Recently, a novel approach has been proposed by Salipante et al. [5] based on the frequency-dependent deformation of giant unilamellar vesicles (GUVs). GUVs represent closed lipid bilayer structures with diameters of dozens of micrometers, therefore facilitating direct microscopy-based measurements of the membrane properties [6,7]. In view of their amenability to control the membrane composition and bathing media environment, GUVs are considered as a suitable biomimetic system for studying the physical properties of biomembranes [8,9]. When exposed to AC electric fields, giant vesicles can deform and porate, see e.g. [10–12]. Depending on the alternating field frequency and the conductivities of the solutions on both sides of the membrane, the vesicle can adopt a prolate shape, elongated in the field direction, or an oblate shape, respectively [13]. The frequency at which the prolate-to-oblate transition occurs was found to depend only on the conductivity conditions, the vesicle radius and the membrane capacitance [14]. Because the former two parameters can be experimentally set or measured, the transition frequency can be directly used to determine the membrane capacitance [5].

A further advantage of GUVs over other model membrane systems is that they represent a free-standing, clean of organic impurities membranes, which offer control over the bilayer tension and curvature. On the contrary, lipid bilayers as in supported lipid bilayers (SLB), black lipid membranes (BLM) or nano-sized liposomes and multilamellar vesicles (MLVs) suffer from the disadvantage of side effects incurring from the support (in SLB and MLVs), the presence of solvent molecules (used in the preparation of BLMs), poor stability (BLM), high curvature (as in small unilamellar vesicle suspensions) and tension (all of the above systems). The latter parameter is important as it may modulate the membrane thickness and thus affect the measured capacitance values. As far as GUVs can offer an appropriate model of a tension-free membrane system, the comparison of results obtained from electrochemical experiments with GUVs and with supported or suspended planar lipid bilayers is expected to elucidate the mechanical tension effects on the electrical properties of membranes.

Sugar molecules are recognized as important players in the adaptive mechanisms of plants to environmental stresses such as their protection against drought [15,16]. On the other hand, sugars are widely employed in cryo- and biopreservation of tissues and alimentary products

[17]. Their cryoprotective and biopreservative efficiency is expected to be strongly dependent upon the molecular mechanisms of interaction with lipid membranes and the alteration of their physicochemical properties by the presence of sugars. Current reports on the effect of sugar molecules on the bending rigidity of membranes are somewhat controversial (e.g. see the discussion in [18]). Trends found for bilayer lipid stacks [19] differ from those measured on free-standing lipid membranes [20–22]. Taking into account that the effect of carbohydrates on the electrical properties of membranes had not been explored yet, we investigate here the influence of sugar concentration on the membrane capacitance as assessed from the method of vesicle electrodeformation. This method has already been applied predominantly to polymer vesicles (one lipid composition was also tested) [5]. The reported results acquired from the analysis of GUV electrodeformation are discussed in the light of membrane-tension effects and the influence of sugar molecules on the studied electrical properties of lipid bilayers.

## 2. Materials and methods

### 2.1. Materials and vesicle preparation

The electroformation method [23] was applied for the preparation of giant unilamellar vesicles from 1-palmitoyl-2-oleoyl-sn-glycero-3-phosphocholine (POPC, Avanti Polar Lipids Inc. AL, USA). Two indium tin oxide (ITO)-coated glass plates, separated by a polydimethylsiloxane (PDMS, Dow Corning, Germany) spacer [24] served as electrodes. A small amount ( $\sim 50 \mu\text{g}$ ) of POPC with concentration of 1 g/L in chloroform-methanol solvent (9:1 volume parts) was spread on the ITO-coated side of each of the electrodes. After the complete evaporation of organic solvents under vacuum, the electroformation chamber was assembled so that the internal volume ( $\sim 4 \text{ ml}$ ) was completely filled with double-distilled water containing 0.01 mol/L of sodium chloride (NaCl, Sigma-Aldrich, Germany) and the desired concentration of sucrose from 0.025 to 0.2 mol/L ( $\text{C}_{12}\text{H}_{22}\text{O}_{11}$ , Sigma-Aldrich, Germany). A high yield of unilamellar vesicles was obtained after the application of AC voltage ( $\sim 1.5 \text{ V}$  peak-to-peak, 50 Hz) to the chamber for a couple of hours, according to previously established electroformation protocols [24]. In order to achieve the desired conductivity ratio of the aqueous phase inside and outside the vesicles, the NaCl concentration of the suspending aqueous phase was increased to 0.012 mol/L maintaining the same sugar concentration as the aqueous solution used for the preparation of GUVs. All aqueous solutions were prepared with double-distilled water from a quartz distiller. Their conductivities were measured with Cyberscan PC510 (Eutech, Singapore).

### 2.2. Vesicle observation and capacitance measurements

Two parallel glass slides, separated by a 0.5 mm-thick (CoverWell®) spacer (Sigma-Aldrich Inc., USA) formed the chamber for vesicle electrodeformation needed to measure the membrane capacitance. A pair of two rectangular parallel to each other ITO-electrodes deposited on the inner surface of the lower glass slide at a distance of 1 mm apart ensured the application of the alternating sine voltage not exceeding 7 V rms from a generator (33120A, HP/Agilent, CA, USA). The studied frequency range was from 0.5 to 1000 kHz. The AC fields in our experiment were below the critical values for membrane electroporation [25]. The vesicle electrodeformation was observed and recorded using the phase-contrast regime of an inverted microscope Axiovert 100 (Zeiss, Germany) equipped with a dry objective ( $\times 63$ , numerical aperture 0.75) and a CCD camera (C3077, Hamamatsu Photonics, Japan) connected to the video input of a frame grabber board (DT3155, Data Translation, USA), mounted in a computer for the digitization of the recorded video signal in  $768 \times 576$  eight-bit pixel format (0.172  $\mu\text{m}/\text{pixel}$ ).

Data analysis was carried out as discussed below following the original approach of Salipante et al. [5]. Recent theoretical and

experimental studies [12–14] reported shape transformations of GUVs upon the application of AC field at varied frequency depending on the ratio  $\Lambda$  between the conductivity  $\lambda_{in}$  of the aqueous solution, enclosed by the vesicle membrane, and the conductivity  $\lambda_{out}$  of the suspending medium [5,11]:

$$\Lambda = \lambda_{in}/\lambda_{out} \quad (1)$$

As far as all experiments were performed under the condition of higher electrical conductivity of the suspending medium, we consider a vesicle in an aqueous solution more conductive than the inner fluid enclosed by the vesicle membrane. In this case  $\Lambda < 1$  and the vesicle shape changes from prolate to oblate with increasing the field frequency. During this morphological transition, the intermediate (critical) frequency,  $f_{cr}$ , at which the vesicle with radius  $r$  assumes its quasi-spherical shape, is given by [14,26]:

$$f_{cr} = \frac{\lambda_{in}}{2\pi r C_m} [(1-\Lambda)(\Lambda + 3)]^{-1/2} \quad (2)$$

where  $C_m$  stands for the specific capacitance of the membrane.

The experimental procedure consisted in recording the frequency-dependent deformation of vesicles. Note that the vesicle excess area (and tension) cannot be controlled during GUV electroformation. Thus, during electrodeformation the vesicles from the same batch adopt shapes of different aspect ratios. From the image sequence taken at every imposed frequency of the AC field, the degree of deformation was measured in order to determine the critical frequency for each of the recorded vesicles. The data acquired for the critical frequencies versus the inverse vesicle radius was afterwards fitted with the theoretical expression (1) taking into account the known values of  $\lambda_{in}$  and  $\Lambda$  for the aqueous solutions in each series of experiments. As a result, the value of the specific capacitance of the membrane was calculated from the fit.

### 3. Results and discussion

#### 3.1. Dependence of the membrane capacitance on sugar concentration

We report the values of the electric capacitance of palmitoyl-oleoyl phosphatidylcholine bilayers in aqueous solutions of 12 mmol/L NaCl containing different concentrations of sucrose ranging from 0 up to 0.2 mol/L. For every sugar concentration, data were acquired from an ensemble of dozens of vesicles from different preparation batches in order to avoid possible artifacts from sample preparations. The equilibrium radius of each studied vesicle was independently determined before the application of the electric field using in-house software for image treatment. The analysis is based on contour detection of the vesicle at a given number of angular directions (64 or 128) and the subsequent calculation of the mean radius in every direction averaged over all accepted contours from the image sequence [27].

The frequency-dependent deformation of the studied vesicles was recorded as sequences of phase-contrast micrographs at given frequencies of the applied alternating field (Fig. 1). At low field frequencies, the vesicle adopts a prolate shape with the long axis parallel to the field direction. This is because the membrane is an insulator and the tangential electric field squeezes the vesicle at the equator and pulls at the poles. At higher field frequencies and when the internal conductivity is lower than the external one, the vesicle adopts an oblate shape. This is due to the surface net charges accumulated across the membrane which compress the vesicle in the axis parallel to the field.

In all experiments reported here, the conductivity of the internal medium was lower than its value for the suspending medium, i.e.  $\Lambda < 1$ , as a result of which the vesicles undergo a prolate-to-oblate transition with increasing the frequency of the AC field. The transition occurs at the frequency value  $f_{cr}$  as demonstrated in Figs. 1 and 2. From the analysis of the image sequences we obtained the axes  $a$  and  $b$  and subsequently the degree of deformation  $a/b$  for each vesicle recorded in the whole range of the AC field frequencies studied. For each vesicle,

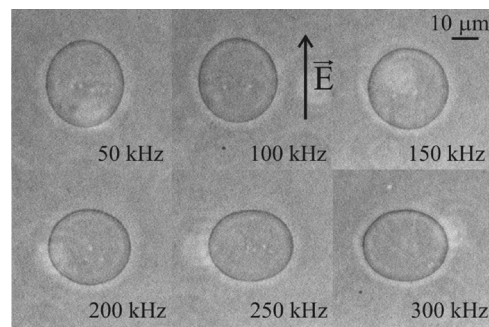


Fig. 1. Phase-contrast images of a POPC vesicle (radius  $r = 18 \mu\text{m}$ ) in 0.2 mol/L of sucrose at different frequencies of the AC field with strength 6 kV/m. The conductivity ratio is  $\Lambda = 0.87$  with internal solution conductivity of 1.48 mS/cm and external solution conductivity of 1.70 mS/cm (the experiment was performed at decreasing the field frequency).

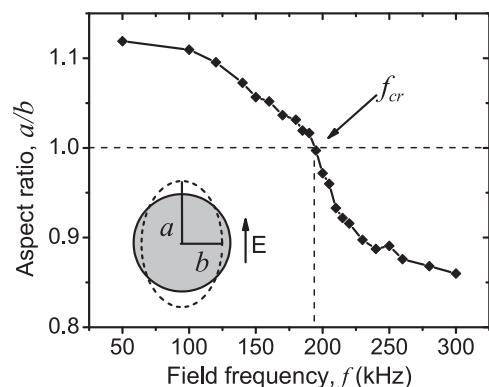


Fig. 2. Deformation of a POPC vesicle with radius of  $18 \mu\text{m}$  in aqueous solution containing 0.2 mol/L of sucrose, as a function of the electric field frequency. The conductivity ratio is  $\Lambda = 0.87$  with sodium chloride concentrations of 0.01 mol/L and 0.012 mol/L inside and outside the vesicle, respectively. The critical field frequency  $f_{cr}$  is obtained from the cross point with the aspect ratio  $a/b = 1$  at which the transition of prolate to oblate shape occurs. For this vesicle, we obtain  $f_{cr} = 190 \text{ kHz}$ .

the aspect ratio  $a/b$  was plotted as a function of frequency as shown in Fig. 2. From interpolation of the measured deformation rate  $a/b$  versus frequency the critical frequency was determined as the cross point with aspect ratio of one for every vesicle from the ensemble (Fig. 2).

#### 3.2. Bare lipid membrane capacitance

The obtained specific capacitances together with the error calculated from the fit of our experimental data for every sugar concentration are summarized in Table 1. The value  $C_m$  represents the resultant capacitance of a series of three capacitors, including the bare lipid bilayer,  $C_B$ , and the capacitances of the space charge regions in the aqueous solution at the two sides of the bilayer, denoted as,  $C_{D,in}$  and  $C_{D,ex}$ :

$$C_m = (1/C_B + 1/C_{D,in} + 1/C_{D,ex})^{-1} \quad (3)$$

The specific capacitance  $C_B$  of the membrane, which on the length scale of a cell-size vesicle of radius  $\sim 10 \mu\text{m}$  is considered as a two-dimensional surface with dielectric permittivity  $\epsilon_B = \epsilon_{rB} \epsilon_0$  ( $\epsilon_{rB}$  stands for the relative dielectric constant of the bilayers and  $\epsilon_0 \approx 8.85 \times 10^{-12} \text{ F/m}$  is the vacuum permittivity) and thickness  $d \sim 5 \text{ nm}$  ( $d \ll r$ ) [12] is given by:

$$C_B = \epsilon_B/d \quad (4)$$

The contribution of  $C_{D,in}$  and  $C_{D,ex}$  is more significant at lower salt concentrations as well as for high enough values of the bilayer

**Table 1**

Specific capacitance of POPC membranes in aqueous solutions with increasing sucrose concentrations obtained from the experiment (see text); GF – goodness of fit. The errors in  $C_m$  and  $C_B$  are standard deviations.

Sucrose, mmol/L	$\lambda_{in}$ , mS/cm	$\Lambda$	$C_m$ , $\mu\text{F}/\text{cm}^2$ (number of vesicles)	$C_B$ , $\mu\text{F}/\text{cm}^2$	GF
0	1.27	0.86	$0.50 \pm 0.02$ (18)	$0.51 \pm 0.02$	0.57
25	1.60	0.84	$0.51 \pm 0.03$ (12)	$0.53 \pm 0.03$	0.68
50	1.21	0.84	$0.55 \pm 0.04$ (33)	$0.58 \pm 0.04$	0.22
100	1.56	0.85	$0.69 \pm 0.05$ (9)	$0.72 \pm 0.05$	0.85
200	1.48	0.87	$0.77 \pm 0.05$ (15)	$0.81 \pm 0.05$	0.83

capacitance as discussed in [5]. In a simplified analysis of our experimental data the capacitance of the electric double layers is taken as the capacitance of a planar capacitor with the dielectric constant of the aqueous solution  $\epsilon_r \approx 80$  [28] and thickness equal to the Debye length,  $\lambda_D$ . The latter is related to the molar concentration  $c$  of a 1:1 electrolyte by the expression  $\lambda_D = 0.303 / \sqrt{c}$  nm [29]. For the concentrations of NaCl applied here, the values of  $\lambda_D$  for the internal solution and the suspending medium were estimated at  $\lambda_D^i = 3$  nm and  $\lambda_D^e = 2.8$  nm, respectively. Using these values we obtained the capacitance for the double layers of free charges in the aqueous solution on both sides of the bilayer  $C_{D,in} = 29 \mu\text{F}/\text{cm}^2$  and  $C_{D,ex} = 27 \mu\text{F}/\text{cm}^2$ .

Therefore, for the salt concentrations of the aqueous solutions used in the present study the contribution of the capacitances due to the space charge regions in the aqueous solution at the two sides of the bilayer is negligible ( $\sim 5\%$ ), see Table 1.

### 3.3. Experimental accuracy analysis

For all values of sucrose concentration studied, the conductivities  $\lambda_{in}$  of the aqueous solution, enclosed by the vesicle membrane, and  $\lambda_{out}$  of the suspending medium (as well as the conductivity ratio  $\Lambda$ ) were the same for all recorded and analyzed vesicles in one batch. The fit of the acquired experimental data for  $f_{cr}$  dependence on the inverse radii of vesicles was performed for fixed  $\lambda_{in}$  and  $\Lambda$ . Thus, the membrane capacitance served as a single fitting parameter. For each sugar concentration, we have examined between 9 and 33 vesicles. Examples for the data in the absence of sugar and in 0.2 mol/L sucrose are given in Fig. 3 with the respective linear fits following Eq. (1). The raw data for the other studied sucrose concentrations with fits are presented in the Supplementary material. The data appears scattered due to the influence of the bulk conductivities on the accuracy of the experimental data as discussed in [5] taking into account the sensitivity of the critical (transition) frequency to the errors in determining the conductivities. Sources of such errors could be uncontrolled evaporation or possible

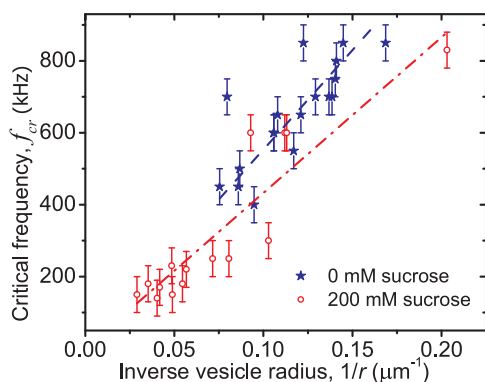


**Fig. 3.** The critical frequencies of prolate-oblate transition for POPC vesicles studied in the absence and presence of sugar. The lines represent data fits with Eq. (1) using the independently measured values of the conductivities  $\lambda_{in}$ ,  $\lambda_{out}$  (i.e.  $\Lambda$ ), and the vesicle radius  $r$ .

vesicle rupture during preparation and handling of vesicle suspensions. The solutions were isotonic to ensure constant volume and the internal conductivity did not change upon preparation of vesicle suspensions. Measures were taken during all manipulations to prevent solvent evaporation. Salipante et al. [5] estimated the errors in the internal conductivity to be of the order of 20–30% compared to the original solution in which vesicles were grown due to possible vesicle rupture during preparation and handling of the vesicle suspensions. We performed error propagation analysis which showed that the error of a single measurement could reach 30–50% due to the above-mentioned uncertainty in  $\lambda_{in}$  (see Eq. (2)). Consequently, for the smallest data set of 9 vesicles analyzed here (see Table 1), the maximum error in the calculated capacitance value is evaluated at  $\sim 17\%$ .

Note also that the approach in Ref. [5] was applied predominantly to polymer membranes, which are characterized by higher thickness (and thus smaller capacitance). This resulted in artificially smaller apparent scatter of the capacitance measurement of the lipid membrane.

### 3.4. Relating the measured capacitance with changes in the membrane thickness

Comparing the capacitance values obtained in sugar-free aqueous solutions  $C_m = 0.50 \pm 0.02 \mu\text{F}/\text{cm}^2$  to the values acquired from experiments with planar lipid membranes [30–35] (see also the data overview in Ref. [36]) we can conclude that our result obtained from measurements on GUVs yields lower specific capacitance compared to the range  $0.55\text{--}1 \mu\text{F}/\text{cm}^2$  reported for planar bilayers of different composition and charge. One major difference between fluctuating vesicles and planar lipid bilayers is that the former represent a low-tension membrane model [27,37] in contrast to the latter, for which the lateral tension is orders of magnitudes higher [38,39]. This tension difference leads, among others, to reduced membrane thickness. The membrane thinning effect on the membrane capacitance has been recently studied by patch-clamp experiments on GUVs in 0.2 mol/L sucrose and glucose solutions [36]. They have shown that the membrane capacitance can vary with tension by up to 3%. However, the measurements were performed in the relatively high-tension regime of mN/m [36]. Here, we employed fluctuating free-floating vesicles with very low membrane tensions,  $10^{-6} \div 10^{-4}$  mN/m as assessed from fluctuation spectroscopy [37,40] (see Supplementary material). The capacitance measurements in our work involve vesicle electrodeformation and thus the membrane tensions are slightly elevated and on the order of  $10^{-3}$  mN/m [12,14,40], which is orders of magnitude lower than the mN/m tensions applied in [36]. Indeed, our results for the capacitance of POPC vesicles are not very far from those measured for membranes of similar thickness (e.g. stearylloleoylphosphatidylcholine:cholesterol 7:3) [36]. Even though the tension ranges in the present study and in [36] differ, the results reported by Garten et al. [36] support the conclusion that the tension associated membrane thinning only partially explain the differences when comparing capacitance data acquired from planar bilayers and from GUVs. Further below, we also explore the possibility of changes in the bilayer dielectric constant as a factor affecting the membrane capacitance.

The specific capacitance is found to increase with increasing the sugar concentration in the aqueous surroundings as shown in Fig. 4. For the maximum sugar concentration of 0.2 mol/L studied here, the measured POPC capacitance ( $0.77 \pm 0.05 \mu\text{F}/\text{cm}^2$ ) is in very good agreement with the capacitance values obtained in Ref. [36] for SOPC and DOPC bilayers for the same concentrations of sucrose and glucose.

The specific capacitance value obtained for 0.2 mol/L of sucrose is approximately 50% higher than the value measured in sugar-free aqueous solutions. We speculated that the reason for this behavior is associated with thinning of the membrane in the presence of sugars. Indeed, small-angle neutron scattering (SANS) measurements on phosphatidylcholine bilayers [41] revealed membrane thinning at sugar concentrations below 0.2 mol/L. As follows from the definition of

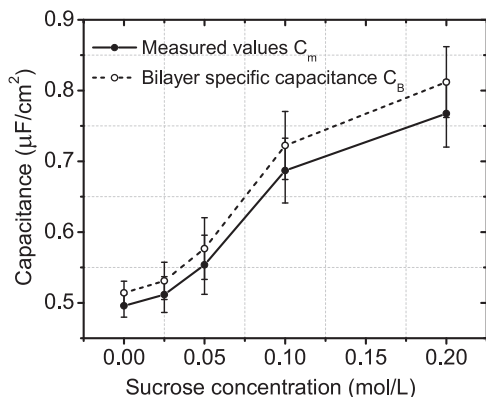


**Fig. 4.** Membrane specific capacitance obtained from electrodeformation of POPC vesicles as a function of the sucrose concentration in water and  $0.84 \leq \Lambda < 0.87$ .

the membrane capacitance, Eq. (3), such membrane thinning is expected to result in increasing values of  $C_m$  as demonstrated by our results. We thus set to explore whether the measured increase in the specific capacitance quantitatively follows the trend in membrane thinning. Assuming that the dielectric permittivity  $\epsilon_B$  remains constant (see Supplementary material), we find that the obtained trend in the membrane capacitance values in water and in sucrose aqueous solutions is stronger than the trend expected solely from membrane thinning ( $\sim 10\%$ ). The non-linear dependence of the electric capacitance on the membrane thickness is shown in Fig. 5. For this plot, we used data for the thickness of dioleoylphosphatidylcholine (DOPC) bilayers at different sugar concentrations obtained from SANS measurements [41]. This is a good approximation as DOPC and POPC bilayers are known to have similar hydrophobic length (at 30 °C, the hydrophobic thickness of DOPC was reported to be between 27.1 Å and 27.2 Å [42–44] and that of POPC was found to be 27.1 Å [45]) and the head groups of these two lipids are identical. The SANS data for the membrane thickness reported by Andersen et al. [41] was measured in the presence of trehalose, but the effects of sucrose were found to be similar as reported in the same reference, presumably because of the similar size and structure of the two sugar molecules.

### 3.5. Assessing the membrane dielectric constant

The obtained data for the membrane capacitance as a function of the membrane thickness (Fig. 5) differs from the expected  $1/d$  dependence (see Eq. (4)). This suggests that the dielectric permittivity of the membrane is also affected by the membrane-sugar interactions. From the obtained capacitance data and the reported membrane thickness, we evaluated the dependence of the relative dielectric permittivity (from Eq. (3)) as a function of sucrose concentration. We find an increase of  $\epsilon_{rB} = \epsilon_B/\epsilon_0$  with increasing sucrose concentration in the aqueous surroundings, Fig. 6. The observed increase is somewhat unexpected as sugars, being hydrophilic molecules, would be intuitively expected to intercalate mainly in the hydrophilic part of the membrane. However, the trend in Fig. 6 suggests that they alter the hydrophobic region as well. We speculate that this results from deeper intercalation of the sucrose molecules into the bilayer. Indeed, molecular dynamics simulations suggest that sugars such as trehalose penetrate deeper in lipid bilayers compared to glucose [47]. Lipid diffusion has also been reported to decrease in the presence of mono- and di-saccharides, which was attributed to hydrogen bonding of sugar molecules to phosphate groups of several lipid molecules [47–49].

It is worth noting that the above estimates for the relative dielectric permittivity are done taking the full thickness of the bilayer. If we take only the thickness of the hydrophobic part of the bilayer, the change is even more pronounced. The thickness of the head group region of

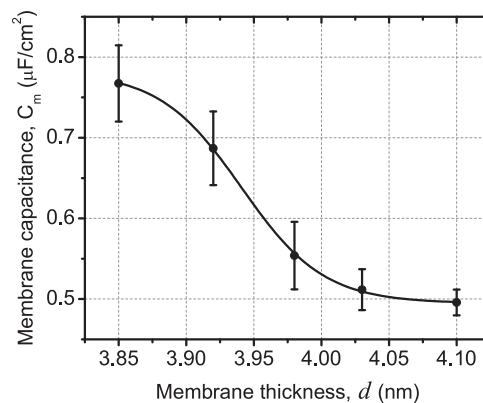


**Fig. 5.** Specific capacitance obtained from electrodeformation of POPC vesicles (measured in this study) as a function of the total bilayer thickness (data from Ref. [41]) at different sugar concentrations, see text for details. The solid curve (a sigmoidal fit) is a guide to the eye.

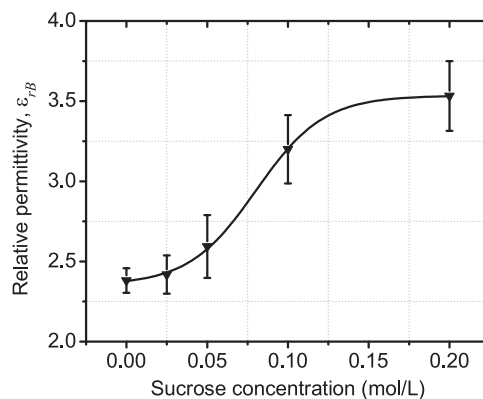


**Fig. 6.** Relative dielectric constant of POPC bilayers obtained from the specific capacitance measured here and the bilayer thickness taken from [41,46] as a function of the sucrose concentration.

phosphatidylcholines is approximately 9 Å [43]. By subtracting the total head group thicknesses of 1.8 nm from the bilayer thickness measured in [41] the relative dielectric permittivity is lowered by more than 40% for increasing sugar concentration and varies between  $\sim 1.3$  and 1.8. In this case, one should keep in mind that the contribution of the headgroup regions must be appropriately taken into account when describing the membrane by an equivalent circuit of capacitors in series.

As mentioned above, SANS studies on membrane-sugar systems [41] have predicted concentration dependent thinning of the bilayer. However, the effect saturates above a certain sugar concentration in the aqueous phase. The dual nature of sucrose-membrane interactions was shown to lead to the strong binding of small carbohydrate molecules at low concentrations, while at higher concentrations sugar molecules gradually become expelled from the membrane surface. Therefore, we performed data fitting with the empirical equation:  $\epsilon_{rB} = \epsilon_{rB}^{max} + (\epsilon_{rB}^{min} - \epsilon_{rB}^{max}) / (1 + \exp(\frac{(c_s - c_0)}{\sigma}))$ . It gives an estimation of the range in which  $\epsilon_{rB}$  varies with the sucrose concentration  $c_s$  taking into account the complex effect of sugar molecules on the bilayer and its saturation as reported in [41]. Here  $c_0 = 0.080 \pm 0.003$  mol/L gives the sugar concentration above which the first derivative of  $\epsilon_{rB}(c_s)$  starts to decrease (towards saturation of the effect).  $\sigma = 0.0209 \pm 0.002$  mol/L represents the slope of the steeper increase of  $\epsilon_{rB}(c_s)$  and could be interpreted as a characteristic sucrose concentration giving an estimation of the strength of the effect. In aqueous solutions without sugar, we estimate the value of  $\epsilon_{rB}^{min} = 2.35 \pm 0.02$ , which is in agreement with the value of  $\sim 2.2$  for the relative dielectric

constant of lipid bilayers found in the literature [25,50–52]. With increasing the sugar concentration, the relative dielectric constant of the membrane increases to the value of  $\epsilon_{rB}^{max} = 3.53 \pm 0.03$ .

### 3.6. Correlation between the electrical and mechanical properties of membranes

The present study provides experimental evidences about the influence of small carbohydrates such as sucrose on the electrical properties of lipid bilayers. We questioned whether the observed dependencies correlate with other material properties of the membrane. For example, the membrane elasticity as characterized by the bending rigidity is known to be relatively sensitive to various compounds present in the membrane and in the solutions [7]. However, the effect of sugars on the membrane bending rigidity has been controversial. While data obtained on giant vesicles suggest a dropdown in the bending rigidity with increasing sugar concentrations (demonstrated for sucrose by mechanical micromanipulation of GUVs [20] and (to a somewhat lesser extent) by shape fluctuation analysis of GUVs [22]), diffuse X-ray measurements on bilayer stacks have shown no (or even the reverse) effect [18,19,53]. Critical discussion of effects associated with the different types of measurements and data analysis is included in [53]. Recently, using diffuse X-ray scattering from multilamellar phosphatidylcholine samples Nagle et al. [19] found no systematic change in the bending modulus at relatively high concentrations of mono- and disaccharides in the aqueous phase. The authors discussed in detail the limited control of the effective sugar concentrations between the neighboring bilayers in the stacks as well as the issues related to the compliance of the average sugar concentrations in their experiment to the bulk concentrations in GUVs samples [19]. Small-angle neutron scattering, dialysis and densitometry measurements revealed that sugars may be either bound or expelled from the bilayer depending on the concentration of sugar [41]. Undoubtedly, the controversial role of sugars on the lipid bilayers mechanics reported so far emphasizes the necessity of further investigations of how small carbohydrates influence the membrane physical properties. We believe that apart from the importance of the tilt deformations as discussed in [18], another factor affecting the difference in the results should be probably taken into account, namely that the ratio of lipid-to-sugar concentrations in the two systems (bilayer stacks and giant vesicles) differs by orders of magnitude. Indeed, for bilayer stacks, no direct evidence for the exact sugar concentration between the individual bilayers can be obtained. We thus restrict our further discussion to data collected on giant vesicles.

In previous studies [20,22] evidences were provided about the influence of sugars on the membrane mechanics. Micromanipulation of GUVs [20] has shown that the bending rigidity of lipid bilayers steeply

decreases with increasing the sugar concentration in the aqueous surroundings, see data in Fig. 7. Thermal shape fluctuation spectroscopy of GUVs supported qualitatively the reduction of the membrane bending constant with saturation of the effect at sucrose concentration higher than 0.1 mol/L [22]. The trend was confirmed by micropipette manipulation experiments on GUVs at two different sugar concentrations [21]. Fig. 7 represents a comparison of the effect produced by sugar molecules on the membrane capacitance with the alteration of the membrane bending rigidity reported in [20]. We plotted the bending rigidity  $k_c$  as a function of the sucrose concentration in the aqueous phase. It can be concluded that both the membrane bending elasticity and its electrical capacitance are altered by the presence of sucrose. The degree of this influence is different for the two membrane properties. The membrane capacitance increases with more than 50%, while the reported decrease in the bending rigidity is approximately 20% as obtained from thermal shape fluctuation analysis of GUVs [22]. Micromanipulation studies of GUVs [20] yielded much stronger alteration of the measured  $k_c$  value with increasing sucrose concentration. As discussed earlier [22] this difference can be due to the contribution of the hidden area of the vesicle membrane [54] to the apparent bending modulus, measured with mechanical micromanipulation without “pre-stressing” of vesicles [55] and expected to be lower than the real one. A plausible explanation of the result that the bending modulus obtained from micropipette aspiration without pre-stressing of GUVs, was observed to decrease steeper could be the increase of the hidden area of the vesicle membrane at higher sucrose concentrations. The results reported from fluctuation analysis were obtained whilst taking measures to overcome all known method-related side contributions to the reported values of the membrane bending rigidity, namely, the white noise contribution to the recorded fluctuations of the vesicle membrane; non-stationarity of vesicles due to uncontrolled deflation during measurements or non-uniformity of the mean vesicle radius over all angular directions [22,27].

## 4. Conclusion

The specific electrical capacitance of phosphatidylcholine membranes in sugar-containing aqueous medium was acquired from the analysis of the frequency-dependent deformation of cell-size lipid vesicles in alternating field. The conductivity of the internal solution (enclosed by the vesicle membrane) was lower than the conductivity of the suspending aqueous phase. Taking into account the membrane-thinning effect of sugars reported in the literature, the value obtained in the presence of sugar is expectedly higher than the specific capacitance reported for vesicles in sucrose-free aqueous medium. Experimental evidences are provided about the influence of small carbohydrates such as sucrose on the electrical properties of lipid bilayers. The difference between the membrane capacitance for GUVs and the value measured for planar bilayers is discussed in the context of the significantly different characteristic ranges of membrane tensions in the two types of experimental systems. The obtained membrane capacitance as a function of the membrane thickness suggests that the dielectric permittivity of the membrane is also affected by the membrane-sugar interactions. From the capacitance data and the reported membrane thickness, the values of the relative dielectric permittivity are evaluated to vary from  $\sim 2.3$  (without sugar) to  $\sim 3.5$  (for sucrose concentrations above  $\sim 0.2$  mol/L).

## Acknowledgements

Financial support from the National Science Fund of Bulgaria (Grant DN08-7/2016) is acknowledged. DM acknowledges TD1104 COST Action-EP4Bio2Med for funding a short-term scientific mission at Max Planck Institute of Colloids and Interfaces. VV and RD acknowledge Petia Vlahovska for useful input and critical reading of the manuscript.

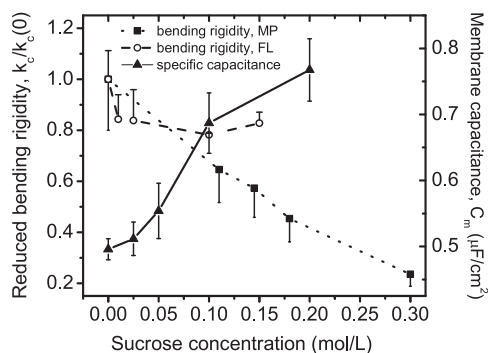


Fig. 7. Bending elasticity (left axis) and specific capacitance (right axis) of phosphatidylcholine membranes in sucrose-containing aqueous solutions; MP denotes micropipette manipulation of GUVs [20]; FL stands for thermal shape fluctuation analysis of GUVs [22]. The bending rigidity was rescaled by the value measured in the absence of sugar.

## Appendix A. Supplementary data

Supplementary material related to this article can be found, in the online version, at doi:<https://doi.org/10.1016/j.colsurfa.2018.05.011>.

## References

- [1] D. Miklavcic, Handbook of Electroporation, Springer International Publishing, 2017 pp. LIII, 2998.
- [2] H.P. Schwan, Dielectrophoresis and rotation of cells, in: E. Neumann, A.E. Sowers, C.A. Jordan (Eds.), Electroporation and Electrofusion in Cell Biology, Springer US, Boston, MA, 1989pp. 3–21.
- [3] K. Kinoshita Jr, I. Ashikawa, N. Saita, H. Yoshimura, H. Itoh, K. Nagayama, A. Ikegami, Electroporation of cell membrane visualized under a pulsed-laser fluorescence microscope, *Biophys. J.* 53 (1988) 1015–1019.
- [4] P. Kramar, D. Miklavcic, M. Kotulska, A. Maček-Lebar, Voltage and current clamp methods for determination of planar lipid bilayer properties, in: A. Iglic (Ed.), Advances in Planar Lipid Bilayers and Liposomes, Elsevier, Academic Press, 2010pp. 29–66.
- [5] P.F. Salipante, R.L. Knorr, R. Dimova, P.M. Vlahovska, Electrodeformation method for measuring the capacitance of bilayer membranes, *Soft Matter* 8 (2012) 3810–3816.
- [6] R. Dimova, S. Aranda, N. Bezlyepkina, V. Nikolov, K.A. Riske, R. Lipowsky, A practical guide to giant vesicles. Probing the membrane nanoregime via optical microscopy, *J. Phys. Condens. Matter* 18 (2006) S1151–S1176.
- [7] R. Dimova, Recent developments in the field of bending rigidity measurements on membranes, *Adv. Colloid Interface Sci.* 208 (2014) 225–234.
- [8] A.G. Petrov, The Lyotropic State of Matter: Molecular Physics and Living Matter Physics, Gordon & Breach, Amsterdam, 1999.
- [9] R. Dimova, Giant Vesicles, A biomimetic tool for membrane characterization, in: A. Iglic (Ed.), Advances in Planar Lipid Bilayers and Liposomes, 2012 Elsevier, Burlington: Academic Press.
- [10] R. Dimova, K.A. Riske, S. Aranda, N. Bezlyepkina, R.L. Knorr, R. Lipowsky, Giant vesicles in electric fields, *Soft Matter* 3 (2007) 817–927.
- [11] R. Dimova, N. Bezlyepkina, M.D. Jordö, R.L. Knorr, K.A. Riske, M. Staykova, P.M. Vlahovska, T. Yamamoto, P. Yanga, R. Lipowsky, Vesicles in electric fields: some novel aspects of membrane behavior, *Soft Matter* 5 (2009) 3201–3212.
- [12] P.M. Vlahovska, R.S. Gracia, S. Aranda-Espinoza, R. Dimova, Electrohydrodynamic model of vesicle deformation in alternating electric fields, *Biophys. J.* 96 (2009) 4789–4803.
- [13] S. Aranda, K.A. Riske, R. Lipowsky, R. Dimova, Morphological transitions of vesicles induced by alternating electric fields, *Biophys. J.* 95 (2008) L19–21.
- [14] T. Yamamoto, S. Aranda-Espinoza, R. Dimova, R. Lipowsky, Stability of spherical vesicles in electric fields, *Langmuir* 26 (2010) 12390–12407.
- [15] H.J. Bohnert, D.E. Nelson, R.G. Jensen, Adaptations to environmental stresses, *Plant Cell* 7 (1995) 1099–1111.
- [16] E.A. Bray, Plant responses to water deficit, *Trends Plant Sci.* 2 (1997) 48–54.
- [17] J.G. Baust, J.M. Baust, Advances in Biopreservation, CRC Press, 2006.
- [18] J.F. Nagle, M.S. Jablin, S. Tristram-Nagle, K. Akabori, What are the true values of the bending modulus of simple lipid bilayers? *Chem. Phys. Lipids* 185 (2015) 3–10.
- [19] J.F. Nagle, M.S. Jablin, S. Tristram-Nagle, Sugar does not affect the bending and tilt moduli of simple lipid bilayers, *Chem. Phys. Lipids* 196 (2016).
- [20] V. Vitkova, J. Genova, M.D. Mitov, I. Bivas, Sugars in the aqueous phase change the mechanical properties of lipid mono- and bilayers, *Mol. Cryst. Liq. Cryst.* 449 (2006) 95–106.
- [21] P. Schelokovskyy, S. Tristram-Nagle, R. Dimova, Effect of the HIV-1 fusion peptide on the mechanical properties and leaflet coupling of lipid bilayers, *New J. Phys.* 13 (2011) 025004.
- [22] D. Mitkova, V. Vitkova, The aqueous surroundings alters the bending rigidity of lipid membranes, *Russ. J. Electrochem.* 52 (2016) 1172–1178.
- [23] M. Angelova, D. Dimitrov, Liposome electroformation, faraday discuss, *Chem. Soc.* 81 (1986) 303–311.
- [24] V. Vitkova, K. Antonova, G. Popkirov, M.D. Mitov, Y.A. Ermakov, I. Bivas, Electrical resistivity of the liquid phase of vesicular suspensions prepared by different methods, *J. Phys. Conf. Ser.* 253 (2010) 012059.
- [25] D. Needham, R.M. Hochmuth, Electro-mechanical permeabilization of lipid vesicles. Role of membrane tension and compressibility, *Biophys. J.* 55 (1989) 1001–1009.
- [26] P.M. Vlahovska, Nonequilibrium dynamics of lipid membranes: deformation and stability in electric fields, in: C.V.K. Aleš Iglič, Michael Rappolt (Eds.), Advances in Planar Lipid Bilayers and Liposomes, Elsevier, Academic Press, Burlington, 2010pp. 101–146.
- [27] J. Genova, V. Vitkova, I. Bivas, Registration and analysis of the shape fluctuations of nearly spherical lipid vesicles, *Phys. Rev. E* 88 (2013) 022707.
- [28] J.O.M. Bockris, S.U.M. Khan, The Interphasial Structure, Surface Electrochemistry: A Molecular Level Approach, Springer US, Plenum Press, New York, 1993 pp. 59–210.
- [29] J.N. Israelachvili, Intermolecular and Surface Forces, Academic Press, New York, 1985.
- [30] O. Alvarez, R. Latorre, Voltage-dependent capacitance in lipid bilayers made from monolayers, *Biophys. J.* 21 (1978) 1–17.
- [31] R. Benz, K. Janko, Voltage-induced capacitance relaxation of lipid bilayer membranes effects of membrane composition, *Biochimica et Biophysica Acta (BBA) Biomembranes* 455 (1976) 721–738.
- [32] M. Montal, P. Mueller, Formation of bimolecular membranes from lipid monolayers and a study of their electrical properties, *Proc. Natl. Acad. Sci. U. S. A.* 69 (1972) 3561–3566.
- [33] O. Batishchev, A. Indenbom, Alkylated glass partition allows formation of solvent-free lipid bilayer by Montal-Mueller technique, *Bioelectrochemistry* 74 (2008) 22–25.
- [34] B. Schuster, D. Pum, O. Braha, H. Bayley, U. Sleytr, Self-assembled  $\alpha$ -hemolysin pores in an S-layer-supported lipid bilayer, *Biochim. Biophys. Acta* 1370 (1998) 280–288.
- [35] L. Gross, A. Heron, S. Baca, M. Wallace, Determining membrane capacitance by dynamic control of droplet interface bilayer area, *Langmuir* 27 (2011) 14335–14342.
- [36] M. Garten, L.D. Mosgaard, T. Bornschlög, S. Dieudonné, P. Bassereau, G.E.S. Toombes, Whole-GUV patch-clamping, *Proc. Natl. Acad. Sci. U. S. A.* 114 (2017) 328–333.
- [37] M.D. Mitov, J.F. Faucon, P. Meleard, P. Bothorel, G.W. Gokel (Ed.), Thermal Fluctuations of Membranes, JAI Press Inc., Greenwich, 1992pp. 93–139.
- [38] G.J. Taylor, G.A. Venkatesan, C.P. Collier, S.A. Sarles, Direct in situ measurement of specific capacitance, monolayer tension, and bilayer tension in a droplet interface bilayer, *Soft Matter* 11 (2015) 7592–7605.
- [39] P.J. Beltramo, R.V. Hooghten, J. Vermant, Millimeter-area, free standing, phospholipid bilayers, *Soft Matter* 12 (2016) 4324–4331.
- [40] R.S. Gracia, N. Bezlyepkina, R.L. Knorr, R. Lipowsky, R. Dimova, Effect of cholesterol on the rigidity of saturated and unsaturated membranes: fluctuation and electrodeformation analysis of giant vesicles, *Soft Matter* 6 (2010) 1472–1482.
- [41] H.D. Andersen, C. Wang, L. Arleth, G.H. Peters, P. Westh, Reconciliation of opposing views on membrane–sugar interactions, *Proc. Natl. Acad. Sci. U. S. A.* 108 (2011) 1874–1878.
- [42] S. Tristram-Nagle, H.I. Petrache, J.F. Nagle, Structure and interactions of fully hydrated dioleoylphosphatidylcholine bilayers, *Biophys. J.* 75 (1998) 917–925.
- [43] J.F. Nagle, S. Tristram-Nagle, Structure of lipid bilayers, *Biochimica et Biophysica Acta* 1469 (2000) 159–195.
- [44] Y. Liu, J.F. Nagle, Diffuse scattering provides material parameters and electron density profiles of biomembranes, *Phys. Rev. E* 69 (2004) 040901(R).
- [45] N. Kucerka, S. Tristram-Nagle, J.F. Nagle, Structure of fully hydrated fluid phase lipid bilayers with monounsaturated chains, *J. Membr. Biol.* 208 (2005) 193–202.
- [46] N. Kučerka, M.-P. Nieh, J. Katsaras, Fluid phase lipid areas and bilayer thicknesses of commonly used phosphatidylcholines as a function of temperature, *Biochimica et Biophysica Acta (BBA) Biomembranes* 1808 (2011) 2761–2771.
- [47] Gvd. Bogaart, N. Hermans, V. Krasnikov, A.Hd. Vries, B. Poolman, On the decrease in lateral mobility of phospholipids by sugars, *Biophys. J.* 92 (2007) 1598–1605.
- [48] A.K. Sum, R. Faller, J.Jd. Pablo, Molecular simulation study of phospholipid bilayers and insights of the interactions with disaccharides, *Biophys. J.* 85 (2003) 2830–2844.
- [49] M.K. Doeven, J.H.A. Folgering, V. Krasnikov, E.R. Geertsma, Gvd. Bogaart, B. Poolman, Distribution, lateral mobility and function of membrane proteins incorporated into giant unilamellar vesicles, *Biophys. J.* 88 (2005) 1134–1142.
- [50] R. Fettiplace, D.M. Andrews, D.A. Maydon, The thickness composition and structure of some lipid bilayers and natural membranes, *J. Membr. Biol.* 5 (1971) 277–296.
- [51] W. Huang, D.G. Levitt, Theoretical calculation of the dielectric constant of a bilayer membrane, *Biophys. J.* 17 (1977) 111–128.
- [52] J.P. Dilger, S.G.A. McLaughlin, T.J. McIntosh, S.A. Simon, The dielectric constant of phospholipid bilayers and the permeability of membranes to ions, *Science* 206 (1979) 1196–1198.
- [53] J.F. Nagle, Introductory lecture: basic quantities in model biomembranes, *Faraday Discuss.* 161 (2013) 11–29.
- [54] V. Vitkova, J. Genova, I. Bivas, Permeability and the hidden area of lipid bilayers, *Eur. Biophys. J.* 33 (2004) 706–714.
- [55] K. Olbrich, W. Rawicz, D. Needham, E. Evans, Water permeability and mechanical strength of polyunsaturated lipid bilayers, *Biophys. J.* 79 (2000) 321–327.

## SUPPLEMENTARY MATERIAL

Sucrose solutions alter the electric capacitance and dielectric permittivity of lipid bilayers,  
V. Vitkova, D. Mitkova, K. Antonova, G. Popkirov and R. Dimova

### *Measurement of the membrane tension*

We performed thermal shape fluctuation analysis to obtain the membrane tension of giant unilamellar vesicles. As described below, the experimental set-up differs from the set-up for electrodeformation experiments. Consequently, fluctuation analysis was not performed for every vesicle but only for several from the same batch to control their quasisphericity and deflation [1] (vesicles with similar visible fluctuations and sizes were explored for the capacitance measurements). The fluctuation analysis is based on contour detection of the vesicle at a given number of angular directions (64 or 128) and the subsequent calculation of the normalized instantaneous angular autocorrelation function  $\xi(\gamma, t)$  of the vesicle radius [1-3]. Considering the radius-vector of a point at the surface of the vesicle in the direction determined by its spherical coordinates  $(\theta, \varphi)$  we can write its small deviation at the moment  $t$  in spherical coordinates as follows:

$$(\theta, \varphi, t) = R_0[1 + u(\theta, \varphi, t)], \quad (\text{S1})$$

with  $R_0$  denoting the radius of a sphere with the same volume as the volume of the vesicle and  $u(\theta, \varphi, t)$  being the normalized function, describing the shape fluctuations. The fluctuations can be decomposed in a series of spherical functions [4]:

$$u(\theta, \varphi, t) = \sum_{n=2}^{n_{max}} \sum_{j=-n}^n U_i^j(t) Y_i^j(\theta, \varphi). \quad (\text{S2})$$

The mean square value of the fluctuations depends on the number  $n$  only, and is given by Milner and Safran [5] considering all modes as independent and applying the equipartition theorem:

$$\langle |U_n^m(t)|^2 \rangle = \frac{k_B T}{k_c} Q^{-1}(\bar{\sigma}, n), \quad (\text{S3})$$

where,  $k_B$  is the Boltzmann constant,  $T$  is the absolute temperature,  $\bar{\sigma} = \sigma R^2/k_c$  is the dimensionless membrane tension, and  $Q(\bar{\sigma}, n) = (n-1)(n+2)[\bar{\sigma} + n(n+1)]$ .

From Equation (S3), it follows that the product

$$\langle |U_n^m(t)|^2 \rangle Q(\bar{\sigma}, n) = \frac{k_B T}{k_c} \quad (\text{S4})$$

does not depend on  $n$  and  $\bar{\sigma}$  and this fact was used for the determination of the (very small and otherwise immeasurable) membrane tension  $\sigma$ , by treating it as an adjustable parameter in the Legendre analysis of the autocorrelation function of the vesicle contour [2, 4].

Sample observation and registration was performed in phase contrast with an inverted Axiovert 100 (Zeiss, Germany) microscope equipped with an oil-immersed objective (100x, NA 1.25). A CCD camera (C3582, Hamamatsu Photonics, Japan) was mounted on the microscope

and connected to the video input of a frame grabber board (DT3155, Data Translation, USA) installed in a computer for the digitization of the registered video signal in 768x576 8-bit pixel format with 0.106  $\mu\text{m}$  pixel size. In order to capture the fastest modes of fluctuation of the vesicular membrane, stroboscopic illumination of the sample was applied using Xenon Flash Lamp (L6604, Hamamatsu, Japan). Images of the equatorial cross-section of the fluctuating vesicle with the focal plane of the objective were acquired in real time (25 frames per second), digitized and recorded on the PC in order to obtain a long image sequence ( $> 10^4$  frames). For the static analysis of membrane fluctuations, i.e. for the deduction of the membrane tension and the bending modulus of the bilayer at free exchange of molecules between the two monolayers, every 25-th frame from the recorded movie was taken. Thus, a new image sequence for the given vesicle was obtained with lapse of one second between two adjacent frames. The image analysis was done as described in [3]. For every vesicle the requirement that the mean radius of the vesicle is constant at all angular directions in the frames of the experimental precision was imposed in order to be considered as stationary and kept for further analysis. After the determination of the  $N$  radius-vectors of the contour, the Fourier amplitudes and the experimental autocorrelation function for each contour from the image sequence were calculated. After its decomposition into a series of Legendre polynomials, the experimental amplitudes for each harmonics were obtained. An important requirement for the goodness of the studied vesicle was the conservation of its volume during the experiment controlled via the evolution of the second harmonics of radius fluctuations [1]. As described in detail in [3] the fitting procedure yielded the bending modulus and the tension of the vesicle membrane with their standard errors. The membrane tensions of free-floating and fluctuating giant vesicles are obtained to range between  $4 \cdot 10^{-6}$  mN/m and  $2 \cdot 10^{-4}$  mN/m. All studied vesicles used for electrodeformation experiments exhibited visible fluctuations (as necessary for fluctuation analysis) in the absence of the electric field. This allows us to conclude that their tensions were in the interval mentioned above.

*Raw data for the critical frequencies as a function of the inverse radii of vesicles*

The ensemble of vesicles studied at every sucrose concentration was characterized by the same conductivity  $\lambda_{in}$  of the aqueous solution, enclosed by the vesicle membrane, and the same conductivity  $\lambda_{out}$  of the suspending medium. Consequently, the ratio  $\Lambda = \lambda_{in}/\lambda_{out}$  was constant for the whole ensemble of vesicles. Therefore, the fit of the data acquired for the intermediate (critical) frequencies,  $f_{cr}$ , described by [6, 7]

$$f_{cr} = \frac{\lambda_{in}}{2\pi r C_m} [(1 - \Lambda)(\Lambda + 3)]^{-1/2}, \quad (\text{S5})$$

was performed with a single free parameter, namely  $C_m$ , standing for the specific capacitance of the membrane by introducing in (S5) the independently measured values of  $\lambda_{in}$  and  $\Lambda$ . The fitting procedure yielded the value of the membrane capacitance with its standard error. The goodness of fit given in Table 1 in the main text is expressed by the value of the adjusted residual  $R^2$ . Figures S1 – S3 show the raw data with their fit for 25, 50 and 100 mmol/L of sucrose. The data for 0 and 200 mmol/L of sucrose are shown in Figure 3 in the main text.

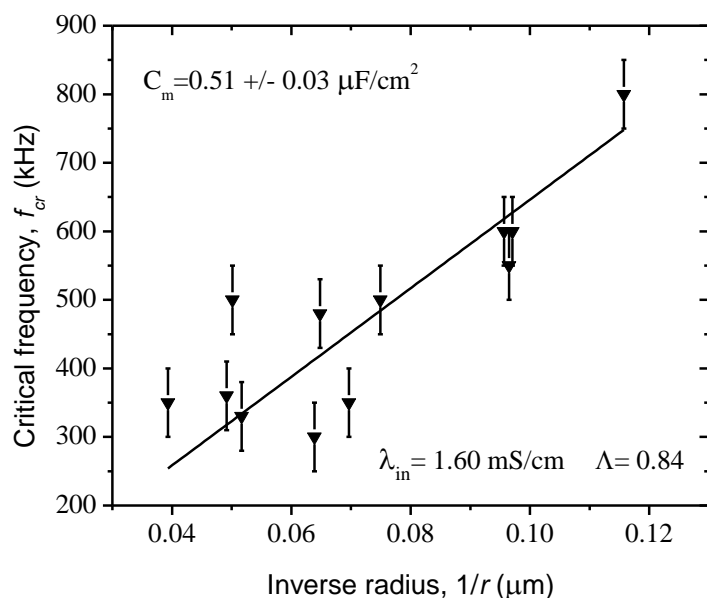


Figure S1. The critical frequencies of prolate-oblate transition for POPC vesicles in 25 mmol/L sucrose solution (10 mmol/L NaCl inside the vesicles and 12 mmol/L NaCl in the suspending medium). The line represents data fit with equation (S5) using the independently measured values of the conductivities  $\lambda_{in}$ ,  $\lambda_{out}$  (i.e.  $\Lambda$ ), and the vesicle radius  $r$ .

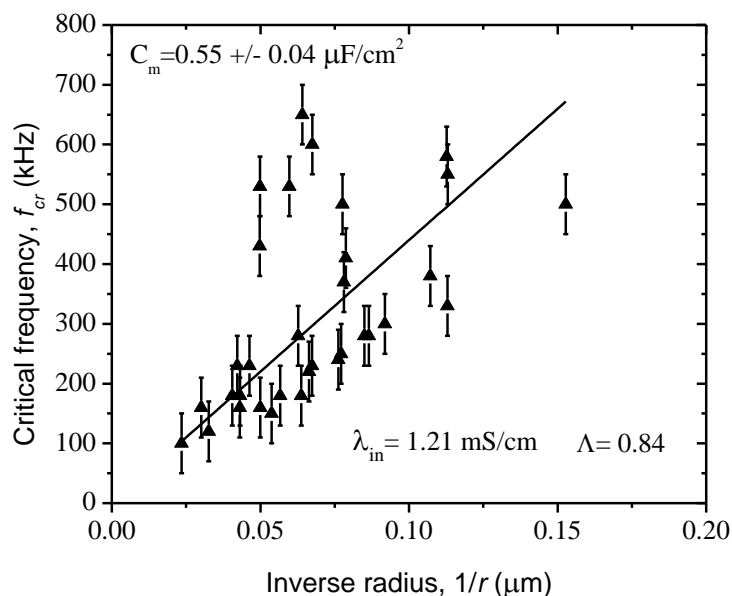


Figure S2. The critical frequencies of prolate-oblate transition for POPC vesicles in 50 mmol/L sucrose solution (10 mmol/L NaCl inside the vesicles and 12 mmol/L NaCl in the suspending medium). The line represents data fit with equation (S5) using the independently measured values of the conductivities  $\lambda_{in}$ ,  $\lambda_{out}$  (i.e.  $\Lambda$ ), and the vesicle radius  $r$ .

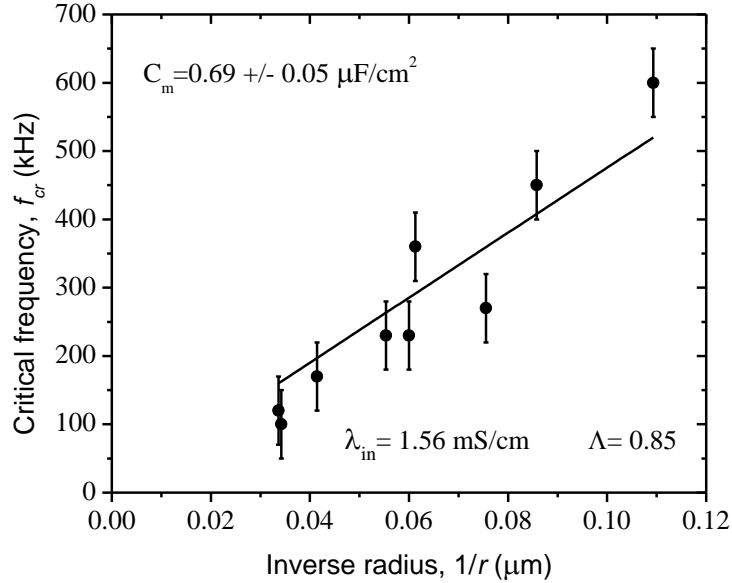


Figure S3. The critical frequencies of prolate-oblate transition for POPC vesicles in 100 mmol/L sucrose solution (10 mmol/L NaCl inside the vesicles and 12 mmol/L NaCl in the suspending medium). The line represents data fit with equation (S5) using the independently measured values of the conductivities  $\lambda_{in}$ ,  $\lambda_{out}$  (i.e.  $\Lambda$ ), and the vesicle radius  $r$ .

#### *Apparent bilayer thickness*

Using the bilayer capacitance values obtained from GUV electrodeformation measurements as a function of the sucrose concentration in the aqueous solution, in Figure S4, we plotted the apparent membrane thickness calculated under the assumption that the dielectric constant of the bilayer is constant and independent on the sugar content:

$$d_{app} = \varepsilon_B / C_B, \quad (\text{S6})$$

where  $\varepsilon_B = \varepsilon_{rB} \varepsilon_0$  with the vacuum permittivity being  $\varepsilon_0 \approx 8.85 \times 10^{-12}$  F/m. We took for the relative dielectric constant of the bilayer  $\varepsilon_{rB} \sim 2.2$  [8-11]. The apparent thickness of the bilayer is obtained to decrease with increasing sucrose concentration in the aqueous solution. This result is not consistent with data for the thickness of phosphatidylcholine bilayers in the presence of sucrose published in the literature [12], which indicates that the assumption for constant dielectric constant of the bilayer is not realistic.

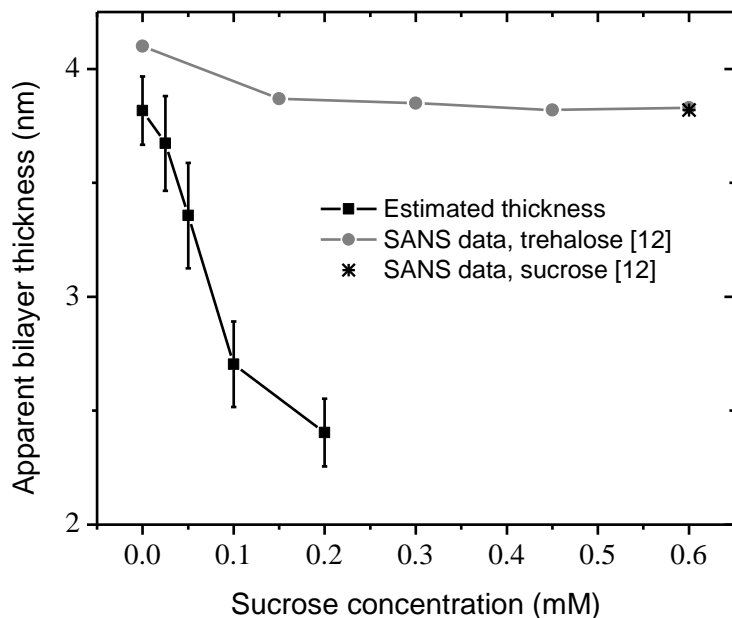


Figure S4. Estimation of the apparent thickness of POPC bilayers from the measured capacitance under the assumption of constant dielectric permittivity of the bilayer. For comparison, data for phosphatidylcholine bilayers in the presence of sucrose and trehalose [12] are also plotted.

#### References:

- [1] V. Vitkova, C. Misbah, Dynamics of lipid vesicles – from thermal fluctuations to rheology, in: A. Iglic (Ed.) *Advances in Planar Lipid Bilayers and Liposomes*, Academic Press, Burlington, 2011, pp. 258-292.
- [2] I. Bivas, P. Hanusse, P. Bothorel, J. Lalanne, O. Aguerre-Chariol, An application of the optical microscopy to the determination of the curvature elastic modulus of biological and model membranes, *J. Physique*, 48 (1987) 855-867.
- [3] J. Genova, V. Vitkova, I. Bivas, Registration and analysis of the shape fluctuations of nearly spherical lipid vesicles, *Physical Review E*, 88 (2013) 022707.
- [4] M.D. Mitov, J.F. Faucon, P. Meleard, P. Bothorel, Thermal fluctuations of membranes, in: G.W. Gokel (Ed.), *JAI Press Inc.*, Greenwich, 1992, pp. 93-139.
- [5] S.T. Milner, S.A. Safran, Dynamical fluctuations of droplet microemulsions and vesicles, *Phys. Rev. A*, 36 (1987) 4371 - 4379.
- [6] T. Yamamoto, S. Aranda-Espinoza, R. Dimova, R. Lipowsky, Stability of spherical vesicles in electric fields, *Langmuir*, 26 (2010) 12390-12407.
- [7] P.M. Vlahovska, Nonequilibrium Dynamics of Lipid Membranes: Deformation and Stability in Electric Fields, in: C.V.K. Aleš Iglič, Michael Rappolt (Ed.) *Advances in Planar Lipid Bilayers and Liposomes*, Elsevier, Academic Press, Burlington, 2010, pp. 101-146.
- [8] R. Fettiplace, D.M. Andrews, D.A. Maydon, The thickness composition and structure of some lipid bilayers and natural membranes, *Journal of Membrane Biology*, 5 (1971) 277-296.
- [9] D. Needham, R.M. Hochmuth, Electro-mechanical permeabilization of lipid vesicles. Role of membrane tension and compressibility, *Biophysical Journal*, 55 (1989) 1001-1009.
- [10] W. Huang, D.G. Levitt, Theoretical calculation of the dielectric constant of a bilayer membrane, *Biophysical Journal*, 17 (1977) 111-128.

- [11] J.P. Dilger, McLaughlin, S. G. A., McIntosh, T. J., and Simon, S. A., The dielectric constant of phospholipid bilayers and the permeability of membranes to ions, *Science*, 206 (1979) 1196-1198.
- [12] H.D. Andersen, C. Wang, L. Arleth, G.H. Peters, P. Westh, Reconciliation of opposing views on membrane–sugar interactions, *Proc Natl Acad Sci U S A*, 108 (2011) 1874–1878.

## SUPPLEMENTARY MATERIAL

Sucrose solutions alter the electric capacitance and dielectric permittivity of lipid bilayers,  
V. Vitkova, D. Mitkova, K. Antonova, G. Popkirov and R. Dimova

### *Measurement of the membrane tension*

We performed thermal shape fluctuation analysis to obtain the membrane tension of giant unilamellar vesicles. As described below, the experimental set-up differs from the set-up for electrodeformation experiments. Consequently, fluctuation analysis was not performed for every vesicle but only for several from the same batch to control their quasisphericity and deflation [1] (vesicles with similar visible fluctuations and sizes were explored for the capacitance measurements). The fluctuation analysis is based on contour detection of the vesicle at a given number of angular directions (64 or 128) and the subsequent calculation of the normalized instantaneous angular autocorrelation function  $\xi(\gamma, t)$  of the vesicle radius [1-3]. Considering the radius-vector of a point at the surface of the vesicle in the direction determined by its spherical coordinates  $(\theta, \varphi)$  we can write its small deviation at the moment  $t$  in spherical coordinates as follows:

$$(\theta, \varphi, t) = R_0[1 + u(\theta, \varphi, t)], \quad (\text{S1})$$

with  $R_0$  denoting the radius of a sphere with the same volume as the volume of the vesicle and  $u(\theta, \varphi, t)$  being the normalized function, describing the shape fluctuations. The fluctuations can be decomposed in a series of spherical functions [4]:

$$u(\theta, \varphi, t) = \sum_{n=2}^{n_{max}} \sum_{j=-n}^n U_i^j(t) Y_i^j(\theta, \varphi). \quad (\text{S2})$$

The mean square value of the fluctuations depends on the number  $n$  only, and is given by Milner and Safran [5] considering all modes as independent and applying the equipartition theorem:

$$\langle |U_n^m(t)|^2 \rangle = \frac{k_B T}{k_c} Q^{-1}(\bar{\sigma}, n), \quad (\text{S3})$$

where,  $k_B$  is the Boltzmann constant,  $T$  is the absolute temperature,  $\bar{\sigma} = \sigma R^2/k_c$  is the dimensionless membrane tension, and  $Q(\bar{\sigma}, n) = (n-1)(n+2)[\bar{\sigma} + n(n+1)]$ .

From Equation (S3), it follows that the product

$$\langle |U_n^m(t)|^2 \rangle Q(\bar{\sigma}, n) = \frac{k_B T}{k_c} \quad (\text{S4})$$

does not depend on  $n$  and  $\bar{\sigma}$  and this fact was used for the determination of the (very small and otherwise immeasurable) membrane tension  $\sigma$ , by treating it as an adjustable parameter in the Legendre analysis of the autocorrelation function of the vesicle contour [2, 4].

Sample observation and registration was performed in phase contrast with an inverted Axiovert 100 (Zeiss, Germany) microscope equipped with an oil-immersed objective (100x, NA 1.25). A CCD camera (C3582, Hamamatsu Photonics, Japan) was mounted on the microscope

and connected to the video input of a frame grabber board (DT3155, Data Translation, USA) installed in a computer for the digitization of the registered video signal in 768x576 8-bit pixel format with 0.106  $\mu\text{m}$  pixel size. In order to capture the fastest modes of fluctuation of the vesicular membrane, stroboscopic illumination of the sample was applied using Xenon Flash Lamp (L6604, Hamamatsu, Japan). Images of the equatorial cross-section of the fluctuating vesicle with the focal plane of the objective were acquired in real time (25 frames per second), digitized and recorded on the PC in order to obtain a long image sequence ( $> 10^4$  frames). For the static analysis of membrane fluctuations, i.e. for the deduction of the membrane tension and the bending modulus of the bilayer at free exchange of molecules between the two monolayers, every 25-th frame from the recorded movie was taken. Thus, a new image sequence for the given vesicle was obtained with lapse of one second between two adjacent frames. The image analysis was done as described in [3]. For every vesicle the requirement that the mean radius of the vesicle is constant at all angular directions in the frames of the experimental precision was imposed in order to be considered as stationary and kept for further analysis. After the determination of the  $N$  radius-vectors of the contour, the Fourier amplitudes and the experimental autocorrelation function for each contour from the image sequence were calculated. After its decomposition into a series of Legendre polynomials, the experimental amplitudes for each harmonics were obtained. An important requirement for the goodness of the studied vesicle was the conservation of its volume during the experiment controlled via the evolution of the second harmonics of radius fluctuations [1]. As described in detail in [3] the fitting procedure yielded the bending modulus and the tension of the vesicle membrane with their standard errors. The membrane tensions of free-floating and fluctuating giant vesicles are obtained to range between  $4 \cdot 10^{-6}$  mN/m and  $2 \cdot 10^{-4}$  mN/m. All studied vesicles used for electrodeformation experiments exhibited visible fluctuations (as necessary for fluctuation analysis) in the absence of the electric field. This allows us to conclude that their tensions were in the interval mentioned above.

*Raw data for the critical frequencies as a function of the inverse radii of vesicles*

The ensemble of vesicles studied at every sucrose concentration was characterized by the same conductivity  $\lambda_{in}$  of the aqueous solution, enclosed by the vesicle membrane, and the same conductivity  $\lambda_{out}$  of the suspending medium. Consequently, the ratio  $\Lambda = \lambda_{in}/\lambda_{out}$  was constant for the whole ensemble of vesicles. Therefore, the fit of the data acquired for the intermediate (critical) frequencies,  $f_{cr}$ , described by [6, 7]

$$f_{cr} = \frac{\lambda_{in}}{2\pi r C_m} [(1 - \Lambda)(\Lambda + 3)]^{-1/2}, \quad (\text{S5})$$

was performed with a single free parameter, namely  $C_m$ , standing for the specific capacitance of the membrane by introducing in (S5) the independently measured values of  $\lambda_{in}$  and  $\Lambda$ . The fitting procedure yielded the value of the membrane capacitance with its standard error. The goodness of fit given in Table 1 in the main text is expressed by the value of the adjusted residual  $R^2$ . Figures S1 – S3 show the raw data with their fit for 25, 50 and 100 mmol/L of sucrose. The data for 0 and 200 mmol/L of sucrose are shown in Figure 3 in the main text.

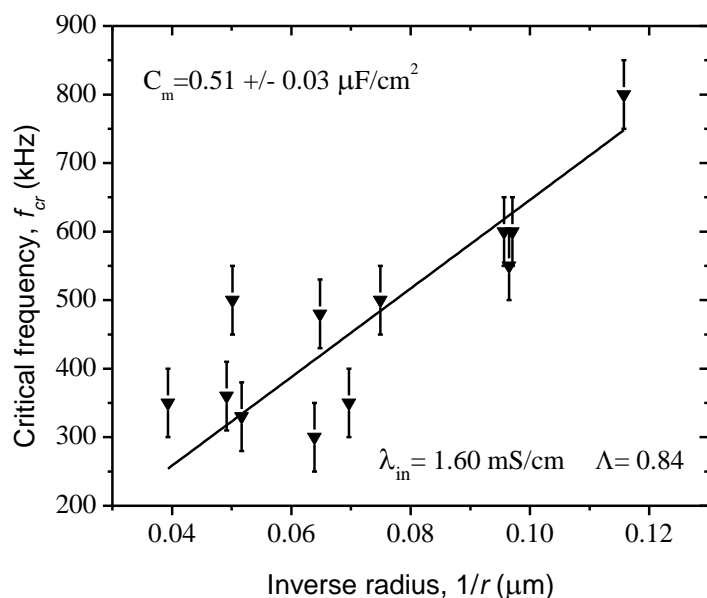


Figure S1. The critical frequencies of prolate-oblate transition for POPC vesicles in 25 mmol/L sucrose solution (10 mmol/L NaCl inside the vesicles and 12 mmol/L NaCl in the suspending medium). The line represents data fit with equation (S5) using the independently measured values of the conductivities  $\lambda_{in}$ ,  $\lambda_{out}$  (i.e.  $\Lambda$ ), and the vesicle radius  $r$ .

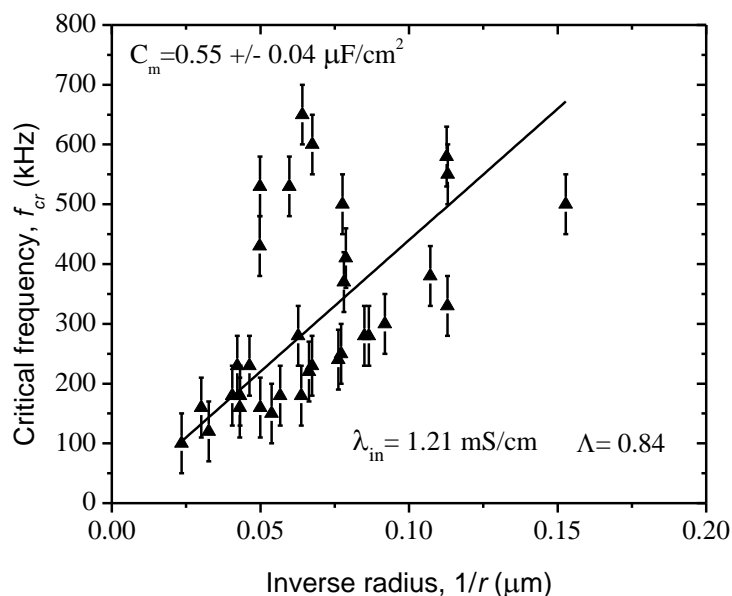


Figure S2. The critical frequencies of prolate-oblate transition for POPC vesicles in 50 mmol/L sucrose solution (10 mmol/L NaCl inside the vesicles and 12 mmol/L NaCl in the suspending medium). The line represents data fit with equation (S5) using the independently measured values of the conductivities  $\lambda_{in}$ ,  $\lambda_{out}$  (i.e.  $\Lambda$ ), and the vesicle radius  $r$ .

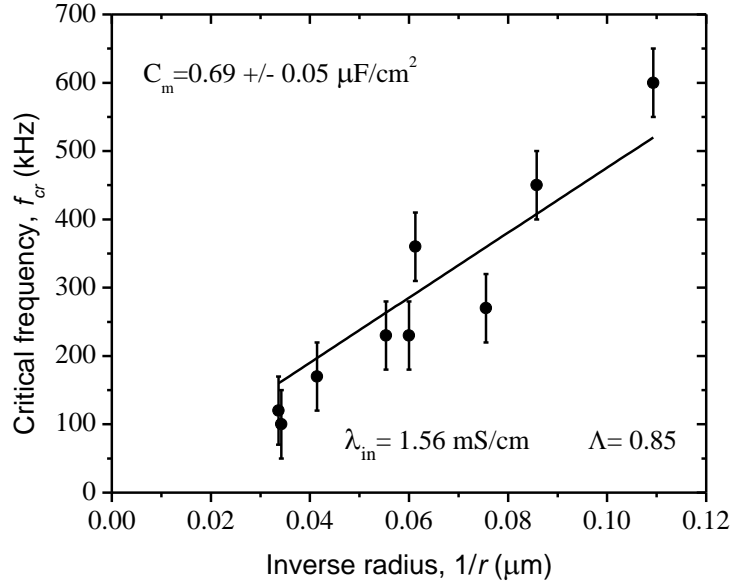


Figure S3. The critical frequencies of prolate-oblate transition for POPC vesicles in 100 mmol/L sucrose solution (10 mmol/L NaCl inside the vesicles and 12 mmol/L NaCl in the suspending medium). The line represents data fit with equation (S5) using the independently measured values of the conductivities  $\lambda_{in}$ ,  $\lambda_{out}$  (i.e.  $\Lambda$ ), and the vesicle radius  $r$ .

#### *Apparent bilayer thickness*

Using the bilayer capacitance values obtained from GUV electrodeformation measurements as a function of the sucrose concentration in the aqueous solution, in Figure S4, we plotted the apparent membrane thickness calculated under the assumption that the dielectric constant of the bilayer is constant and independent on the sugar content:

$$d_{app} = \varepsilon_B / C_B, \quad (\text{S6})$$

where  $\varepsilon_B = \varepsilon_{rB} \varepsilon_0$  with the vacuum permittivity being  $\varepsilon_0 \approx 8.85 \times 10^{-12}$  F/m. We took for the relative dielectric constant of the bilayer  $\varepsilon_{rB} \sim 2.2$  [8-11]. The apparent thickness of the bilayer is obtained to decrease with increasing sucrose concentration in the aqueous solution. This result is not consistent with data for the thickness of phosphatidylcholine bilayers in the presence of sucrose published in the literature [12], which indicates that the assumption for constant dielectric constant of the bilayer is not realistic.

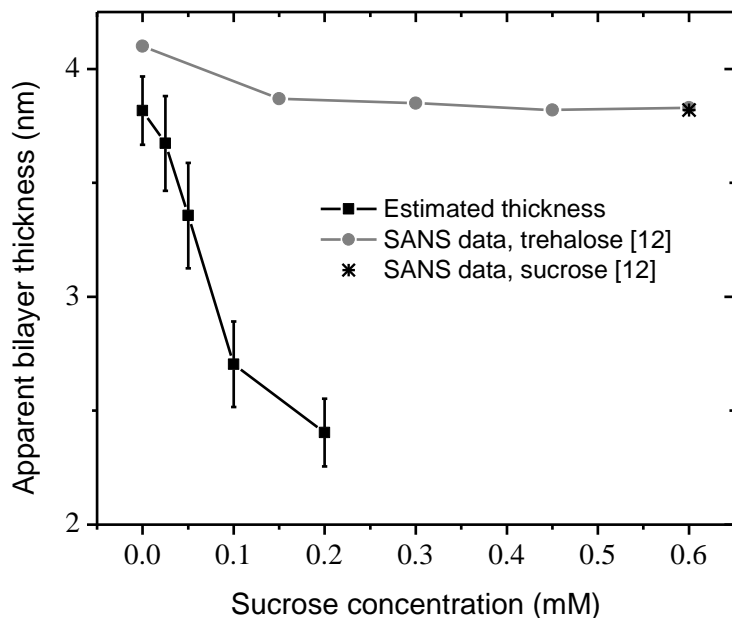


Figure S4. Estimation of the apparent thickness of POPC bilayers from the measured capacitance under the assumption of constant dielectric permittivity of the bilayer. For comparison, data for phosphatidylcholine bilayers in the presence of sucrose and trehalose [12] are also plotted.

#### References:

- [1] V. Vitkova, C. Misbah, Dynamics of lipid vesicles – from thermal fluctuations to rheology, in: A. Iglic (Ed.) *Advances in Planar Lipid Bilayers and Liposomes*, Academic Press, Burlington, 2011, pp. 258-292.
- [2] I. Bivas, P. Hanusse, P. Bothorel, J. Lalanne, O. Aguerre-Chariol, An application of the optical microscopy to the determination of the curvature elastic modulus of biological and model membranes, *J. Physique*, 48 (1987) 855-867.
- [3] J. Genova, V. Vitkova, I. Bivas, Registration and analysis of the shape fluctuations of nearly spherical lipid vesicles, *Physical Review E*, 88 (2013) 022707.
- [4] M.D. Mitov, J.F. Faucon, P. Meleard, P. Bothorel, Thermal fluctuations of membranes, in: G.W. Gokel (Ed.), *JAI Press Inc.*, Greenwich, 1992, pp. 93-139.
- [5] S.T. Milner, S.A. Safran, Dynamical fluctuations of droplet microemulsions and vesicles, *Phys. Rev. A*, 36 (1987) 4371 - 4379.
- [6] T. Yamamoto, S. Aranda-Espinoza, R. Dimova, R. Lipowsky, Stability of spherical vesicles in electric fields, *Langmuir*, 26 (2010) 12390-12407.
- [7] P.M. Vlahovska, Nonequilibrium Dynamics of Lipid Membranes: Deformation and Stability in Electric Fields, in: C.V.K. Aleš Iglič, Michael Rappolt (Ed.) *Advances in Planar Lipid Bilayers and Liposomes*, Elsevier, Academic Press, Burlington, 2010, pp. 101-146.
- [8] R. Fettiplace, D.M. Andrews, D.A. Maydon, The thickness composition and structure of some lipid bilayers and natural membranes, *Journal of Membrane Biology*, 5 (1971) 277-296.
- [9] D. Needham, R.M. Hochmuth, Electro-mechanical permeabilization of lipid vesicles. Role of membrane tension and compressibility, *Biophysical Journal*, 55 (1989) 1001-1009.
- [10] W. Huang, D.G. Levitt, Theoretical calculation of the dielectric constant of a bilayer membrane, *Biophysical Journal*, 17 (1977) 111-128.

- [11] J.P. Dilger, McLaughlin, S. G. A., McIntosh, T. J., and Simon, S. A., The dielectric constant of phospholipid bilayers and the permeability of membranes to ions, *Science*, 206 (1979) 1196-1198.
- [12] H.D. Andersen, C. Wang, L. Arleth, G.H. Peters, P. Westh, Reconciliation of opposing views on membrane–sugar interactions, *Proc Natl Acad Sci U S A*, 108 (2011) 1874–1878.